The current issue and full text archive of this journal is available at
www.emeraldinsight.com/0961-5539.htm

Fast, nonlinear network flow solvers for fluid and thermal transient analysis

Alok K. Majumdar
Thermal Analysis Branch, Propulsion System Department, Engineering Directorate, NASA Marshall Space Flight Center, Huntsville, Alabama, USA, and
S.S. Ravindran
Department of Mathematical Sciences, Shelby Center for Science and Technology, The University of Alabama in Huntsville, Huntsville, Alabama, USA

Received 30 April 2009
Reviewed 5 August 2009
Revised 12 August 2009
Accepted 19 August 2009

Abstract

Purpose – The purpose of this paper is to present a fast nonlinear solver for the prediction of transients in network flows.

Design/methodology/approach – Broyden method-based nonlinear solvers are developed to solve the system of conservation equation for fluids by judiciously exploiting physical coupling among the equations.

Findings – To demonstrate the feasibility and robustness of the solvers, two test cases of practical engineering interest were solved. The results obtained by the solvers were verified against analytical results for a simplified case. The performance of the solvers was found to be comparable or better than existing solvers.

Originality/value – The proposed solver enables predictions of fluid and thermal transients in complex flow networks feasible in reduced computational time.

Keywords Flow, Heat transfer, Fluids

Paper type Research paper

Nomenclature

A	cross-sectional area (ft^2)
A_{cc}	tube cross-sectional area (ft^2)
a	speed of sound (ft/s)
C_f	specific heat of the fluid (Btu/lb °F)
C_L	flow coefficient
C_p	specific heat at constant pressure (Btu/lb °F)
C_w	specific heat of the tube wall (Btu/lb °F)
c	wave speed (ft/s)
D	diameter of the pipe (ft)
f*	Darcy-Weisbach friction factor
g_c	gravitational constant (32.174 lb-ft/lb_f s^2)
h	enthalpy (Btu/lb)
h_c	heat transfer coefficient (Btu/ft^2-s °F)
J	mechanical equivalent of heat (=778 ft-lb_f/Btu)
K_{f*}	flow resistance coefficient (lb_f-s^2/(lb-ft)^2)
K_{rot}	nondimensional rotating flow resistance coefficient
L	length of the tube (ft)
$\dot{m}$	mass flow rate (lb_m/s)
m	resident mass (lb)

The authors are grateful to the Marshall Space Flight Center and the financial support of NASA Grant NNM05AA22A.

International Journal of Numerical Methods for Heat & Fluid Flow
Vol. 20 No. 6, 2010
pp. 617-637

0961-5539
DOI 10.1108/09615531011056791

N_{Re}	Reynolds number
n	number of branches
O	order
p	pressure (lb_f/ft^2)
$\dot{Q}$	heat source (Btu/s)
R	gas constant (lb_f-ft/lb-°R)
r	radius (ft)
S	momentum source (lb_f)
T	temperature (°F)
T_f	fluid temperature (°F)
T_w	wall temperature (°F)
t	time (s)
V	volume (ft^3)
v	fluid velocity (ft/s)
z	compressibility factor
δ	tube wall characteristic length (ft)
ε	surface roughness of pipe (ft)
ρ_f	fluid density (lb/ft^3)
ρ_w	tube wall density (lb/ft^3)

Subscripts

i	ith node
ij	branch connecting nodes i and j
j	jth node
u	upstream

1. Introduction

The computation of fluid flow in network consisting of both systems and components is of significant importance in engineering and industry such as design and operation of rocket propulsion systems(Majumdar and Steadman, 2001), design of natural gas and water distribution (Osiadacz, 1988), and design of air flow through a gas turbine combustor (Stuttaford and Rubini, 1996). Most of the existing network flow analysis methods deal mainly with specific flows such as flow in pipelines, incompressible flows, slightly compressible flows, or isothermal flows. They also use the pressure correction technique proposed in Patankar and Spalding (1972) for their computation (Greyvenstein and Laurie, 1994).

In Majumdar (1999), a novel finite, volume-based network flow analysis procedure that is capable of analyzing unsteady compressible flows in complex networks involving both components and systems is described. It uses a "staggered grid" technique (Patankar, 1980) and solves the discrete coupled nonlinear conservation equations simultaneously by using Newton's method. Newton's method is computationally costly for large-scale flow network problems involving large numbers of nodes and branches. The major part of the computational (CPU) effort comes from the computation and inversion of the Jacobian matrix.

Another method suitable for solving discrete nonlinear conservation equations is the Broyden's method (Broyden, 1965). In Broyden's method, one replaces the Jacobian matrix with a suitable approximate Jacobian matrix and updates it as iteration progresses. The latter update procedure has the advantage of not having to use Gaussian elimination to solve the linear algebraic system. Broyden's method is fast and suitable for computing transient problems and problems that require computation in a long time interval.

The application that motivated the present work is the modeling and prediction of fluid and thermal transients encountered in the design and operation of rocket propulsion systems. Fluid transients such as rapid valve closure and priming of evacuated feed lines significantly influence the design and operation of both spacecraft and launch vehicle propulsion systems. Fluid transients occur at system activation and shutdown in rocket propulsion systems. Due to ground safety requirements many

spacecraft are launched without any propellant and they are evacuated while reaching the orbit. Pressure surges are created during propulsion system activation and shutdown due to valve opening and closure, respectively. These pressure surges must be predicted accurately to ensure structural integrity of the propulsion system fluid network. The method of characteristics (MOC) is a popular method for computing fluid transients in straight pipeline (Wylie and Streeter, 1982; Chaudhry, 1979; Moody, 1990). MOC is a semi-analytical technique that solves the mass and momentum conservation equations along the characteristics. However, this technique is limited to simple systems such as straight pipelines and certain constraints involving the relative value of the time step to the space step, making it computationally expensive. The chilldown of fluid transfer lines is common in the operation of a cryogenic propulsion system such as those found in spacecraft and missiles. The chilldown of cryogenic transfer lines is a complex, unsteady heat transfer problem involving rapid heat exchange from a solid structure to a fluid with phase change as well as pressure fluctuations. It is of great interest as it directly impacts the design of delivery systems for the propellant. The prediction of chilldown time, temperature, and pressure during the chilldown process for a given transfer line is of interest in cryogenic operation. Prediction of chilldown time requires modeling and understanding of transient heat transfer phenomena. Several analytical and numerical studies on chilldown of cryogenic transfer lines have been reported in the literature (Cross *et al.*, 2002; Chi, 1965; Steward *et al.*, 1970). In Chi (1965), an analytical model of the chilldown under the assumption of constant flow rate, heat transfer coefficient, and fluid properties can be found. In Steward *et al.* (1970), a numerical modeling of a one-dimensional chilldown process was presented using a finite difference method. In Cross *et al.* (2002), finite volume-based numerical modeling was presented for prediction of the chilldown of a cryogenic transfer line, based only on transient heat transfer effects and neglecting fluid transient effects.

In this paper, some Broyden method-based nonlinear solvers are presented for solving the system of conservation equations for network flows by judiciously exploiting physical coupling among the equations. Numerical methods for solving the nonlinear, fully coupled system of algebraic equations arising from network flow models can be classified into two broad classes:

(1) fixed-point iteration, also known as successive substitution method; and

(2) Newton's method, which is a simultaneous solution method.

In certain applications, the coupling among mass conservation, momentum conservation, and equation of state is stronger than other equations such as the enthalpy equation or specie conservation equation. This coupling among equations is exploited to devise a "divide-and-conquer" strategy whereby the equations that are more strongly coupled are solved by the Newton's method and the equations that are not strongly coupled with the other set of equations are solved by fixed-point iterations. This strategy, as demonstrated in the sequel, leads to significant memory and computer time savings. An added advantage of this "splitting" strategy over the "all-at-once," fully simultaneous strategy is that the fixed-point iteration can be used as an initial guess for the Newton's method, thus improving the convergence characteristics of the Newton's method and the overall algorithm. Therefore, four different solvers are proposed for solving the nonlinear algebraic system of equations:

(1) hybrid Newton-successive substitution (Newton-SS) solver;

(2) Broyden solver;

(3) hybrid Broyden-successive substitution (Broyden-SS); and

(4) Newton solver.

The nonlinear solver proposed in Majumdar (1999) and Cross *et al.* (2002) used a combination of the successive substitution method and the Newton's method (Newton-SS) to solve the nonlinear systems.

The proposed nonlinear solver's ability to fast and accurately predict fluid transients is demonstrated in numerical prediction of chilldown in cryogenic transfer lines and pressure surges during rapid valve opening without heat transfer.

2. Network finite volume formulation

The analysis of the flow distribution in a complex flow network requires modeling of the system using boundary nodes, internal nodes, and branches. The flow domain is divided into a discrete number of control volumes and the conservation equations of mass, momentum, and energy are determined for each control volume. At boundary nodes, pressures and temperatures are prescribed. At internal nodes, pressures and temperatures are computed by solving time-dependent mass and energy conservation equations. Each internal node is a control volume where there are inflow and outflow of mass and energy at the boundaries of the control volume. The discretization scheme assumes that the flow is driven by the pressure differential between the upstream and downstream nodes. This is known as the "staggered grid" technique that is popular in solving Navier-Stokes equations by the finite volume method (Patankar, 1980).

Mass and energy conservation equations are solved at the internal nodes in conjunction with thermodynamic equation of state. Flow rates are computed at the branches by solving the time-dependent momentum conservation equation. This process of discretization allows the development of the set of conservation equations in an unstructured coordinate system. Figure 1 displays a schematic showing adjacent nodes, their connecting branches, and the indexing system used by the network solver.

2.1 Mass conservation equation

The mass conservation equation at the *i*th node can be expressed as:

$$\frac{(m_i)_{t+\Delta t} - (m_i)_t}{\Delta t} = -\sum_{j=1}^{j=n} \dot{m}_{ij}. \tag{1}$$

Equation (1) requires that, for the transient formulation, the net mass flow from a given node must equate to the rate of change of mass in the control volume.

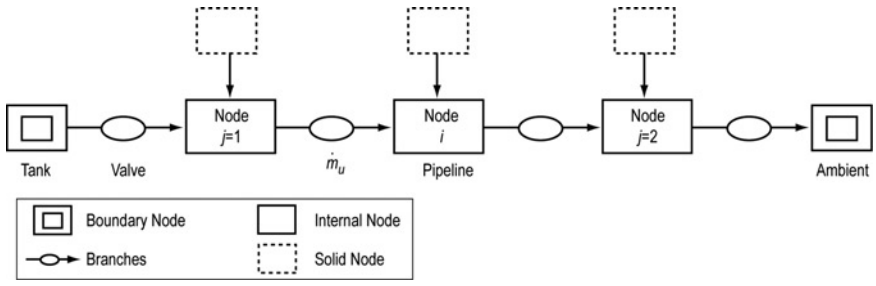

Figure 1.
Schematic of GFSSP nodes, branches, and indexing practice

2.2 Energy conservation

The energy conservation equation for node i, shown in Figure 1, can be expressed following the first law of thermodynamics and using enthalpy as the dependent variable. It can be written as:

$$\frac{m\left(h-\frac{p}{\rho J}\right)_{t+\Delta t}-m\left(h-\frac{p}{\rho J}\right)_{t}}{\Delta t}=\sum_{j=1}^{j=n}\{\max[-\dot{m}_{ij},0]h_j-\max[\dot{m}_{ij},0]h_i\}+\dot{Q}_i. \quad (2)$$

Equation (2) shows that for transient flow, the rate of increase of internal energy in the control volume is equal to the rate of energy transport into the control volume minus the rate of energy transport from the control volume plus any external rate of heat transfer from the surroundings ($\dot{Q}_i$). One example is solid-to-fluid heat transfer that is further described in section 4.

The max operator used in equation (2) is known as an upwind differencing scheme that has been extensively employed in the numerical solution of Navier-Stokes equations in convective heat transfer and fluid flow applications. When the flow direction is not known, this operator allows the transport of energy only from its upstream neighbor. In other words, the upstream neighbor influences its downstream neighbor but not vice versa.

2.3 Momentum conservation equation

The flow rate in a branch is calculated from the momentum conservation equation (equation (3)) that represents the balance of fluid forces acting on a given branch:

$$\begin{aligned}&\frac{(mu)_{t+\Delta t}-(mu)_t}{g_c\Delta t}+\max[\dot{m}_{ij},0](u_{ij}-u_u)-\max[-\dot{m}_{ij},0](u_d-u_{ij})\\&\quad=(p_i-p_j)A_{ij}-K_{f*}\dot{m}_{ij}|\dot{m}_{ij}|A_{ij}.\end{aligned} \quad (3)$$

A typical branch configuration is shown in Figure 2. Inertia, pressure, and friction are considered in the conservation equation. It should also be noted that the flow rate ($\dot{m}$) is a vector quantity. A negative value of $\dot{m}_{ij}$ signifies that the flow is directed from the jth node to the ith node.

The two terms on the left side of the momentum equation represent the inertia of the fluid. The first term is the time-dependent term that must be considered for unsteady calculations. The second term is significant when there is a large change in area or density from branch to branch. The first term on the right side of the momentum equation represents the pressure gradient in the branch. The second term represents the frictional effect. Friction is modeled as a product of K_{f*}, the square of the flow rate, and area. K_{f*} is a function of the fluid density in the branch and the nature of flow passage being modeled by the branch. For a pipe with length (L) and diameter (D), K_{f*} can be expressed as $K_{f^*}=8f^*L/\rho_u\pi^2D^5g_c$.

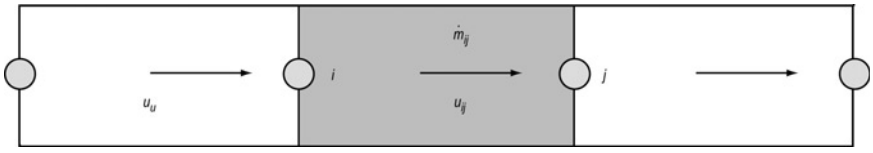

Figure 2.
Schematic of a branch ij with nodes i and j

For a valve, K_{f*} can be expressed as $K_{f^*} = 1/2\rho_u C_L^2 A^2 g_c$. The friction factor f^* in the definition of K_{f*} is calculated from the Colebrook equation (1938-1939), which is expressed as $1/f^* = -2\log\left[\varepsilon/3.7D + 2.51/N_{\mathrm{Re}}\sqrt{f^*}\right]$, where ε is the surface roughness height which is a property of the pipe material.

The momentum conservation equation also requires knowledge of the density and the viscosity of the fluid within the branch. These are functions of the temperatures and pressures, and are provided by the thermodynamic property program GASP (Hendricks *et al.*, 1975) that provides the thermodynamic and transport properties for different fluids.

2.4 Equation of state

Transient flow calculations require the knowledge of resident mass in a control volume. The resident mass in the *i*th control volume is calculated from the equation of state for real fluids:

$$m = \frac{pV}{RTz}. \tag{4}$$

The compressibility factor (z) and temperature (T) in equation (4) are calculated from the thermodynamic property program (Hendricks *et al.*, 1975) for a given pressure and enthalpy. The pressure, enthalpy, and resident mass in internal nodes and the flow rate in branches are calculated by solving the fully coupled, nonlinear system of equations (1), (2), (4), and (3), respectively. There is no explicit equation for pressure. The pressure is calculated implicitly from the mass conservation equation. In section 3, the nonlinear iterative solvers to solve the system equations (1)-(4) are described.

3. Nonlinear solvers

The fully discrete conservation equations (1)-(4) can be written as $F(x) = 0$, where x is the n-dimensional array containing the unknown pressure, temperature, flow rate, mass, and enthalpy. The function $F{:}R^n \rightarrow R^n$ represents the discrete conservation equations (1)-(4). The simplest iterative method for solving a system of nonlinear, simultaneous, algebraic system of equations is the fixed-point iteration or successive substitution method. In this method, the system $F(x) = 0$ is written as $x = G(x)$. x is iteratively computed by solving $x^{k+1} = G(x^k)$ for a given approximate solution x^k. Under suitable assumptions on the function $G(x)$, namely G is differentiable and $\sum_{i=1}^{n}(((\partial G_i(x))/\partial x_j) < 1$, for $k = 1$ to n, at least in the neighborhood of the solution, the approximate solutions x^{k+1} converges within specified tolerance to a solution x and the convergence rate is linear. However, for complex problems, these conditions are very difficult to verify in practice and implementation of safeguards are necessary. If the iterations exhibit oscillatory behavior, a simple way to damp them is to use the linear combination of x^k and x^{k+1}, $\alpha x^k + (1{-}\alpha)\, x^{k+1}$, as the new approximation. In most cases, with a suitable choice of $0 \leq \alpha \leq 1$, convergence can be achieved. However, even if one can find α that would guarantee convergence, the convergence can be very slow with an excessive number of iterations, such is the case with the large-scale, complex flow network computations. If the function $F(x)$ is differentiable, the derivative information can be used for convergence acceleration. Newton's method computes the approximation x^{k+1} by solving $J(x^k)(x^{k+1}{-}x^k) = -F(x^k)$, where $J(x^k)$ is the Jacobian matrix $J(x)_{ij} = ((\partial F_i(x))/\partial x_j)$. Solving this equation requires computing the Jacobian matrix by finite difference approximations and solving the linear algebraic system of equations by Gaussian elimination with partial pivoting. For

smooth functions with an initial guess sufficiently close to the solution, this method has a quadratic convergence rate. However, total CPU cost associated with derivative evaluation and Gaussian elimination is $O(n^3)$ and thus can be prohibitively expensive for large-scale network flow problems involving a large number of nodes and branches.

3.1 Broyden's method

The two CPU-intensive steps of evaluating the Jacobian matrix and inverting it can be done more efficiently by using a multidimensional generalization of the secant method at the cost of superlinear convergence. These methods are known as quasi-Newton methods. In (Broyden (1965), a novel way to approximate the inverse Jacobian was proposed using the Sherman-Morrison formula. In this method, new approximation x^{n+1} is computed by solving $x^{n+1} = x^n - J_n^{-1}F(x^n)$, where $J_n{}^{-1}$ is the approximate Jacobian matrix and is computed by the formula $J_n^{-1} = J_n^{-1} + [(\Delta x^n - J_{n-1}^{-1}\Delta F_n)/((\Delta x^n)^t J_{n-1}^{-1}\Delta F_n)] \times (\Delta x^n)^t J_{n-1}^{-1}$, where $(\Delta x^n)^t$ is the transpose of the correction vector Δx^n.

Broyden's method outlined above requires n function evaluations as opposed to $n^2 + n$ evaluations in Newton's method. Moreover, Newton's method requires solving the linear system involving $O(n^3)$ arithmetic operations, where as Broyden's method requires an update that involves only matrix vector multiplication requiring only $O(n^2)$ arithmetic operations.

3.2 Hybrid methods

Here, the "divide-and-conquer" strategy that exploits the structure of the physical coupling among the conservation equations and the design of a hybrid Newton-fixed-point iteration method is described. Let x_1 denote the array of enthalpy variables of dimension k and x_2 denote the array containing the pressure, mass, and flow rate variables of dimension m, where $m + k = n$. The equation $F(x) = F(x_1, x_2) = 0$ is split into two sets of equations: $f(x_2) = 0$ for the unknown x_1 and $g(x_1, x_2) = 0$ for the unknown x_2. The equation $f(x_2) = 0$ represents the tightly coupled continuity, momentum, and equation of state. The equation $g(x_1, x_2) = 0$ represents the energy equation. In the hybrid Newton-fixed-point iteration, equation $f(x_1) = 0$ is solved by Newton's method and the equation $g(x_1, x_2) = 0$ is solved by fixed-point iteration (successive substitution method). The resulting solver can be summarized as follows:

Set $k = 0$:

- Given x_1^k and x_2^k, x_1^{k+1} by Newton's method: $J(x_1^k)(x_1^{k+1} - x_1^k) = -f(x_1^k)$.
- For $m = 0, 1, 2, \ldots$, compute x_2^{m+1} by successive substitution method:

$$x_2^{m+1} = g(x_1^{k+1}, x_2^m).$$

- Set $x_2^{k+1} = x_2^*(\text{converged } x_2^m)$, $k = k + 1$ and go to (1).

In the hybrid Broyden-fixed-point iteration method, the tightly coupled equations $f(x_1) = 0$ are solved by the Broyden's method and the equation $g(x_1, x_2) = 0$ is solved by successive substitution method. It can be summarized as follows:

Set $k = 0$:

- Given x_1^k and x_2^k, x_1^{k+1} by Broyden's method: $x_1^{k+1} = x_1^k - J_k^{-1}f(x_1^k)$.

- For $m = 0, 1, 2, \ldots$, compute x_1^{m+1} by successive substitution method:

$$x_2^{m+1} = q(x_1^{k+1},\ x_2^m).$$

- Set $x_2^{k+1} = x_2^*(\text{converged}\, x_2^m)$, $k = k + 1$ and go to (1).

In general, Broyden's method may not converge when started far from the solution in some problems. This was the case when Broyden's method was used to solve the sudden valve closure problem presented in section 4. It is therefore necessary to use some globalization (safeguard) technique to guarantee convergence of the method. The simplest precaution is to use $x^{k+1} = x^k + \alpha_k\ \Delta x_k$, where α_k is a scalar parameter and $\Delta x_k = x^{k+1} - x^k$. The parameter α_k reduces the correction Δx_k when it is too large. Line search bracketing is used to select the best α systematically with the help of residual $F(x^k + \alpha_k\ \Delta x_k)$. The basic idea is to use the iteration history to model the scalar function $q(\alpha) = \|F(x^k + \alpha\ \Delta x_k)\|$ with a polynomial whose minimum is taken as the next step length α. A three-point parabolic polynomial model is used for this purpose. If α_c is not acceptable, a model polynomial is constructed and its minimum α_t is computed analytically. Then, α is set as follows:

$$\alpha = \begin{cases} \sigma_0\alpha_c & \text{if } \alpha_t < \sigma_0\alpha_c \\ \sigma_1\alpha_c & \text{if } \alpha_t > \sigma_0\alpha_c \\ \alpha_t & \text{otherwise} \end{cases}.$$

The three-point parabolic polynomial model is constructed as follows. If the full step $x^k + \Delta x_k$ is rejected, $\alpha = \sigma_1$ is set and tried again. If the second step is also rejected, the values $q(0)$, $q(\alpha_c)$, and $q(\alpha_-)$ remain, where α_c and α_- are the most recently rejected values of α. The three-point parabolic polynomial is the interpolation of the data $(0,q(0))$, $(\alpha_c, q(\alpha_c))$, and $(\alpha_-,q(\alpha_-))$. See Kelly (1995) for more details. In implementations here, $\sigma_0 = 1$ and $\sigma_1 = 0.5$ are used.

In section 4, four solvers on two test problems involving fluid and thermal transients in cryogenic pipeline are implemented. The following shortened forms of these four nonlinear solvers are used: Broyden for the simultaneous Broyden solver, Newton for the simultaneous Newton solver, Broyden-SS for the hybrid Broyden-SS solver, and Newton-SS for the hybrid Newton-SS solver. In a typical unsteady calculation, our finite volume flow network procedure carries out the following steps:

(1) At the beginning of a new time step, supply an initial value for all the dependent variables in the flow domain, e.g. pressure, resident mass, density, and enthalpy, at all internal and boundary nodes and flow rates at all branches.

(2) Begin the outer iteration loop; this loop calculates density, temperature, compressibility factor, viscosity, etc. at all internal nodes and flow resistance in the branches.

(3) Solve mass conservation equation (1) in internal nodes, momentum conservation equation (3) in branches, energy conservation equation (2), and equation (4) of resident mass in internal nodes by the Newton/Broyden solver.

(4) This step is carried out only in the hybrid solvers: solve the energy conservation equation by the successive substitution method.

(5) Calculate density and temperature from the equation of state for calculated pressure and enthalpy at each internal node. Viscosity is also computed from the thermophysical property correlation for calculated pressure and temperature.

(6) Calculate flow resistance K_{f*}.

(7) Repeat steps (3)-(6) until the maximum difference is less than the specified tolerance of convergence.

(8) Repeat steps (1)-(7) until final time is reached.

4. Test problems and CPU results

The feasibility and robustness of the proposed solvers will be demonstrated by solving the following two test problems involving transients:

(1) sudden valve closure in a horizontal pipeline; and

(2) chilldown of a cryogenic pipeline.

4.1 Test problem I: fluid transient following sudden valve closure

In this test, liquid oxygen (lox) flows from a tank at the upstream end to the downstream end of a pipeline of constant area. At $t = 0$, a valve located at the downstream end of the pipeline begins to close, which is fully open in the beginning. The physical model is schematically shown in Figure 3. The objective of this problem (Majumdar and Flachbart, 2003) is to be able to predict the liquid's response to the sudden valve closure, including the maximum expected pressure and the frequency of oscillation. The lox flows at 500 psia at a temperature of −260 °F through a 400-ft-long, 0.25-in-diameter pipeline at a mass flow rate of 0.0963 lbm/s. At time zero, a valve at the end of the pipeline begins a 100-ms rapid closure.

In order to apply the network finite volume formulation, the pipeline is discretized into nodes that are connected by branches as shown in Figure 1. The branches are segments of pipeline that can be compared with "reaches" of the MOC. Figure 4 shows the generalized fluid system simulation program (GFSSP) finite volume model of the pipeline and tank. The model consists of 12 nodes and 11 branches. Node 1 is a boundary node representing the propellant tank. The pressure and temperature are prescribed at node 1. Node 12 is also a boundary node representing ambient condition. Nodes 2-11 are internal nodes where pressure and temperature are computed. The first

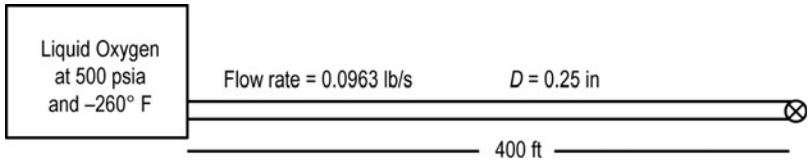

Figure 3.
Schematic of the pipeline connected to a tank with an isolated valve placed at the end

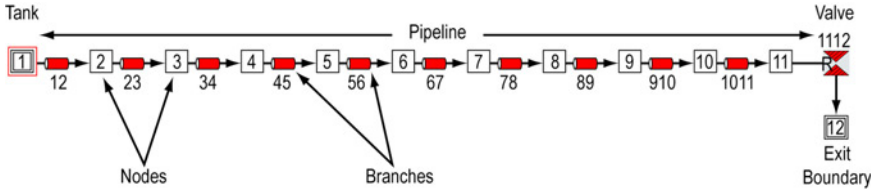

Figure 4.
Finite volume GFSSP model of the flow network with single pipeline and valve

ten branches represent pipe segments, each 40 ft in length. Branch 1,112 represents the valve.

The valve closes in 0.1 s as described in Table I, which is considered rapid closing since the valve closure time is less than the period of oscillation, $2L/a$, where L is the length of the tube and a is the speed of sound. The valve closure history is shown in Table I. The inflow boundary pressure and temperature are kept at 500 psia and $-260\,^{\circ}$F, respectively. The outflow boundary pressure and temperature are kept at 450 psia and $-260\,^{\circ}$F, respectively, so that there is a 50-psia pressure difference in the pipe to drive the flow. In order to obtain the initial conditions, a steady-state flow distribution is first calculated with 450 psia ambient boundary pressures.

4.1.1 Analytical model and solution. For one-dimensional, unsteady flow, the two partial differential equations for mass and momentum conservation in a horizontal pipeline are Wylie and Streeter (1982) and Chaudhry (1979):

$$\frac{\partial p}{\partial t} + \rho c^2 \frac{\partial v}{\partial x} = 0 \tag{5}$$

and

$$\frac{\partial v}{\partial t} + \frac{1}{\rho}\frac{\partial p}{\partial x} + \frac{f*}{2D} v|v| = 0, \tag{6}$$

where v is the fluid velocity inside the pipe, p the pressure, ρ the fluid density, f* the Darcy-Weisbach friction factor, D the diameter of the pipe, and c the wave speed. Equations (5) and (6) form coupled, nonlinear, hyperbolic, partial differential equations.

The MOC solution has been chosen as a benchmark for verification. The MOC is the classical method for calculating fluid transients in straight pipeline (Wylie and Streeter, 1982; Chaudhry, 1979; Moody, 1990). In the MOC (Abott, 1966), these partial differential equations are converted into a system of ordinary differential equations. The following is obtained:

$$C^+ : \ \frac{dv}{dt} + \frac{1}{\rho c}\frac{dp}{dt} + \frac{f^*}{2D} v|v| = 0, \quad \frac{dx}{dt} = c$$

and

$$C^- : \ \frac{dv}{dt} - \frac{1}{\rho c}\frac{dp}{dt} + \frac{f^*}{2D} v|v| = 0, \quad \frac{dx}{dt} = -c,$$

where "+" is for waves coming from upstream, while "−" is for the waves coming from downstream.

These ordinary differential equations can be solved by the finite difference method along the lines of characteristics C^+ and C^-. Integrating these equations along the

Time (s)	Area (in^2)
0	0.0491
0.02	0.0164
0.04	0.0055
0.06	0.0018
0.08	0.0006
0.10	0

Table I.
Valve closure history

characteristic lines between time steps t and $t + \Delta t$ yields:

$$v_j^{n+1} = \frac{1}{2}(v_{j-1}^n + v_{j+1}^n) + \frac{1}{2\rho c}(p_{j-1}^n - p_{j+1}^n) - \frac{\Delta t f^*}{4D}(v_{j+1}^n|v_{j+1}^n| + v_{j-1}^n|v_{j-1}^n|) \quad (7)$$

and

$$p_j^{n+1} = \frac{1}{2}(p_{j-1}^n + p_{j+1}^n) + \frac{\rho c}{2}(v_{j-1}^n - v_{j+1}^n) - \frac{\Delta t f^* c}{4D}(v_{j+1}^n|v_{j+1}^n| - v_{j-1}^n|v_{j-1}^n|), \quad (8)$$

in which ${v^{n+1}}_j$ is the unknown velocity at point x_j at time t_{n+1}, and ${p^{n+1}}_j$ the unknown pressure at point x_j at time t_{n+1}. Discretizing the pipe into segments of length Δx, equations (7) and (8) can be used to calculate the pressure and velocity at all interior points of the pipe. Time step should satisfy the Courant-Friedrichs-Lewy condition for numerical stability which is $Cr = c\Delta t/\Delta x < 1$.

4.1.2 Results. The purpose of the investigation was to show the efficiency and accuracy of the four solvers, and compare its performance with the Newton-SS nonlinear solver proposed in Majumdar (1999). For numerical comparison, the computed pressure at the node immediately behind the valve will be used. Comparison of predicted maximum pressures and period of oscillations between the MOC and the nonlinear network solver is shown in Table II for a finite volume formulation involving 20 branches. Good agreement is shown for the period of oscillation and maximum pressure between the analytical and numerical solutions. However, the accuracy of the numerical results are sensitive to three numerical parameters:

(1) grid size (number of branches);

(2) time step size (Δt); and

(3) tolerance for the residual.

Several CPU experiments to elucidate their effects were performed. In Figures 5-7, the computed results of pressure with the MOC results are compared. In these computations, the tolerance and time step are fixed, and the number of branches is varied, which amounts to increasing the spatial grid resolution. As observed in the figures, increasing the number of branches increases the accuracy of the results. Further improvement in accuracy is obtained by reducing the time step size as seen in Figures 8-10. In Figure 8, unphysical oscillations in the numerical results are shown, especially with the Broyden solvers. However, this numerical artifact disappears with the usage of more branches. Another way to eliminate these unphysical oscillations that does not require an increase in the number of branches is to use smaller tolerances, which is useful if one cannot or does not want to increase the number of branches.

Table II. Maximum pressure and period of oscillation computed by various solvers with 20-branch model

Solver	Maximum pressure (psia)	Period of oscillation (s)
MOC	636	0.65
Newton	618.64	0.646
Broyden	616.59	0.648
Newton-SS	616.17	0.645
Broyden-SS	618.98	0.648

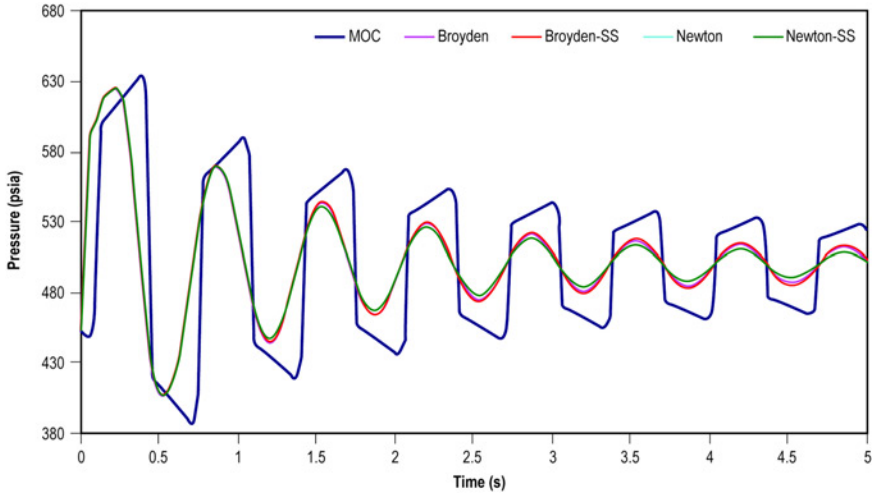

Figure 5.
Five-branch model results with tolerance $= 10^{-8}$ and time step $\Delta t = 0.01$ s

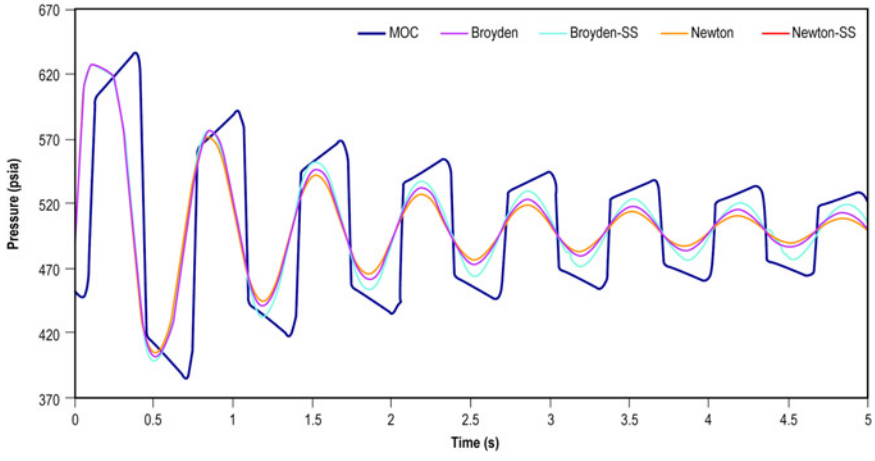

Figure 6.
Ten-branch model results with tolerance $= 10^{-8}$ and time step $\Delta t = 0.01$ s

Figure 11 clearly shows that oscillations in the pressure that are pure numerical artifacts can be successfully eliminated by using tighter tolerance to residual. Experience with the four solvers in this example is that smaller tolerance is generally necessary for convergence and accuracy. This holds true more so for the Broyden solvers than for the Newton solvers. But, CPU experiments with other problems, including the chilldown problem presented next, show too small a tolerance is not necessary for all problems.

Discrepancies, however, exist between the MOC and the four solvers in damping rate and shape of the curve. These are largely due to the way the physics of the flow was modeled in the MOC and network flow solvers. MOC, for example, uses speed of sound in the governing equations, whereas in the network flow solvers, the effect of speed of sound is modeled by the compressibility factor, which is computed from the

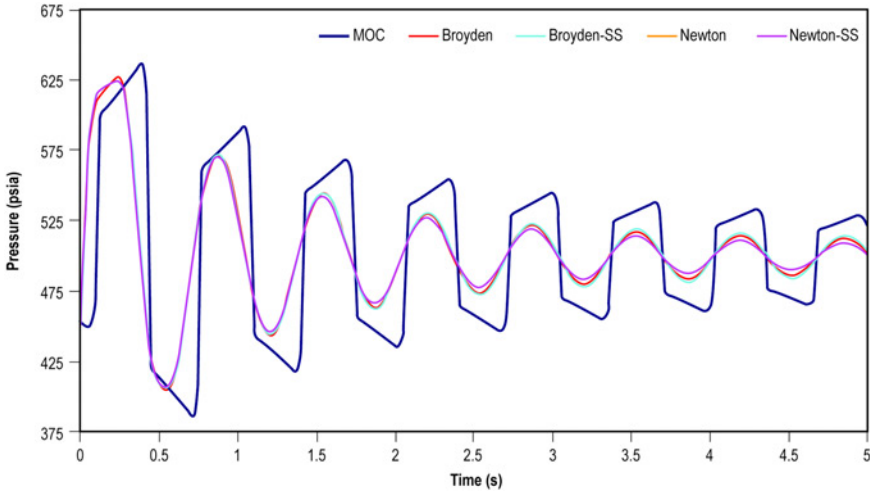

Figure 7.
20-branch model results with tolerance $= 10^{-8}$ and time step $\Delta t = 0.01$ s

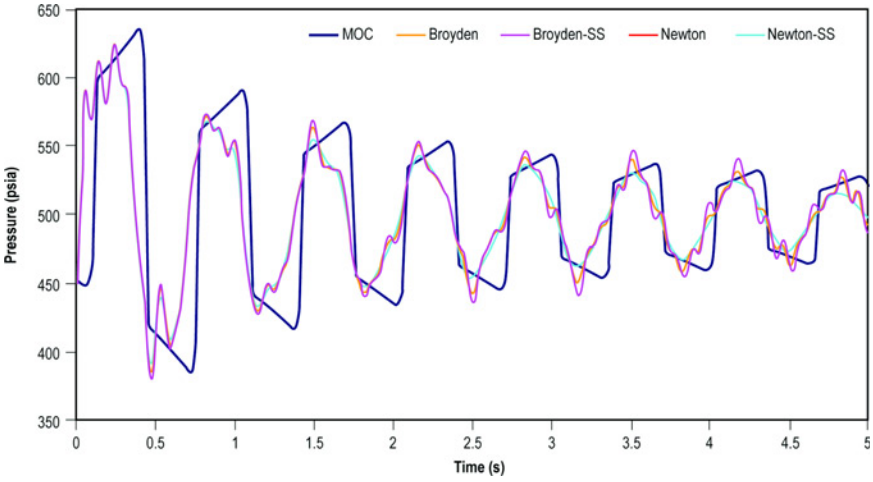

Figure 8.
Five-branch model results with tolerance $= 10^{-8}$ and time step $\Delta t = 0.001$ s

energy equation and equation of state. Also, network flow solvers and MOC use different time steps, and due to this the valve closure history, has not been perfectly matched between the solutions.

Table III shows CPU time for each solver for the time step of $\Delta t = 0.01$ s and Table IV shows similar comparison for the time step of $\Delta t = 0.001$ s. Both tables show CPU time for five-, ten-, and 20-branch models. The CPU savings in the Broyden method is substantial, as seen in both cases. Table III shows that in the 20-branch case, Broyden-SS gives a 42 percent reduction in CPU time over Newton-SS and pure Broyden gives a 61 percent reduction in CPU time in the case of pure Newton solver. Similar reductions are seen in the case of ten and 20 branches. In the ten-branch case, Broyden-SS gives a 56 percent reduction over Newton-SS and Broyden gives a 63 percent reduction over Newton. In the five-branch case, these reductions are 52 and 66 percent, respectively.

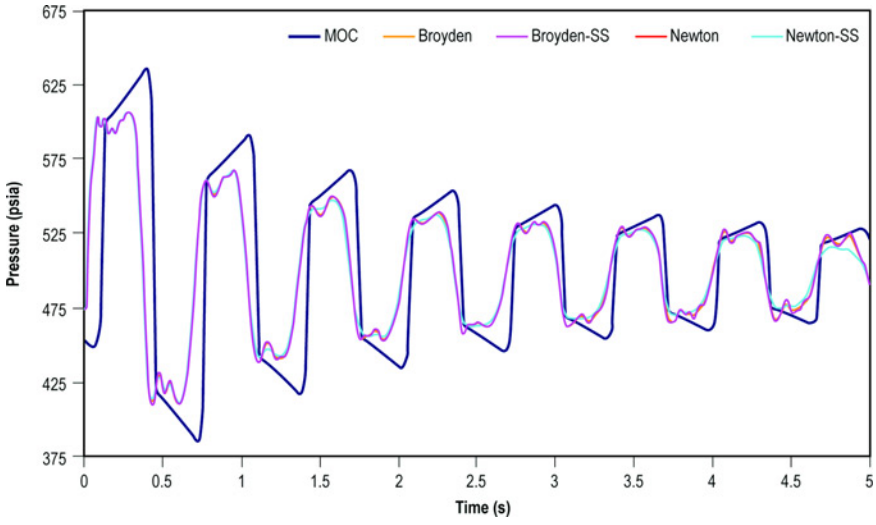

Figure 9.
Ten-branch model results with tolerance $= 10^{-8}$ and time step $\Delta t = 0.001$ s

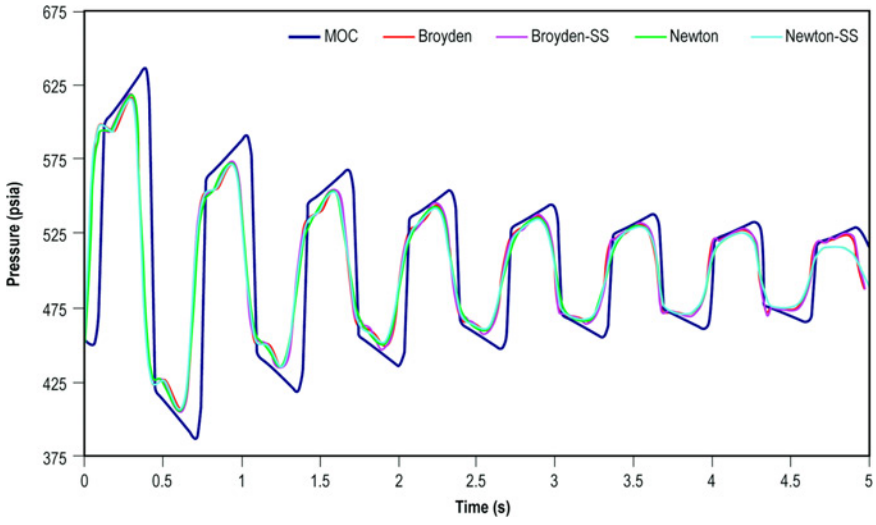

Figure 10.
20-branch model results with tolerance $= 10^{-8}$ and time step $\Delta t = 0.001$ s

Table IV shows that in the five-branch case, Broyden-SS gives a 49 percent reduction in CPU time over Newton-SS, and pure Broyden gives an 83 percent reduction in CPU time in the case of pure Newton solver. Similar reductions are seen in the case of ten and 20 branches. In the ten-branch case, Broyden-SS gives a 46 percent reduction over Newton-SS, and Broyden gives a 77 percent reduction over Newton. In the 20-branch case, these reductions are 44 and 71 percent, respectively.

4.2 Test case II: chilldown of cryogenic pipeline

In this test case, the following conjugate heat transfer problem is solved. Hydrogen gas at cryogenic temperature flows through a tube initially at ambient temperature. The

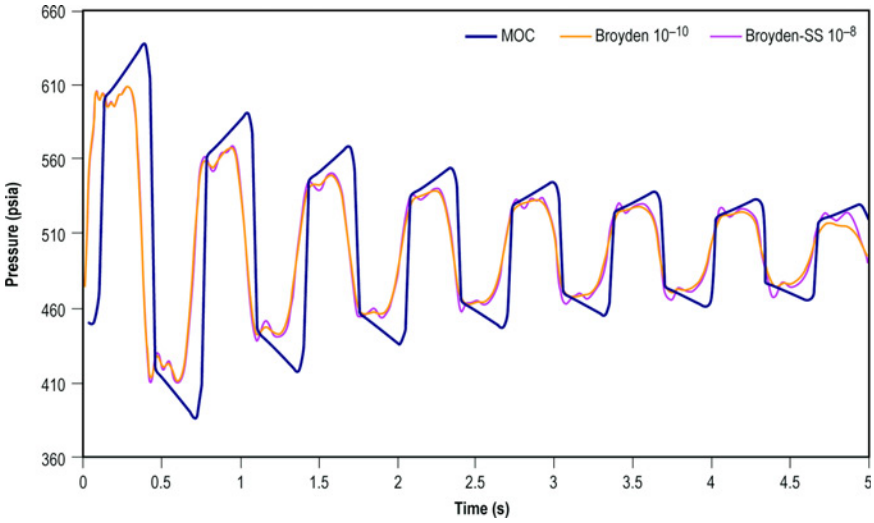

Figure 11.
A ten-branch result that shows the effects of tolerance in mitigating the unphysical oscillations

Method	CPU (5-branch model) (s)	CPU (10-branch model) (s)	CPU (20-branch model) (s)
Broyden-SS	1,136	2,119	5,845
Newton-SS	2,376	4,824	10,094
Newton	3,641	7,613	21,903
Broyden	1,254	2,824	8,667

Table III.
CPU time comparison with various solvers used to solve the rapid valve closure problem with tolerance $=10^{-8}$ and time step size $\Delta t = 0.01$

Method	CPU (5-branch model) (s)	CPU (10-branch model) (s)	CPU (20-branch model) (s)
Broyden-SS	9,109	18,654	49,452
Newton-SS	17,918	34,307	87,411
Newton	35,435	65,222	168,707
Broyden	6,000	14,757	50,078

Table IV.
CPU time comparison with various solvers used to solve the rapid valve closure problem with tolerance $=10^{-8}$ and time step size $\Delta t = 0.001$

physical model is schematically shown in Figure 12. It is of interest to predict how long it takes to chill down a given pipeline. In a fluid-solid network for conjugate heat transfer, solid nodes, ambient nodes, and conductors become part of the flow network. There are four types of conductors:

(1) solid-to-solid conductor;

(2) solid-to-solid radiation conductor;

(3) solid-to-fluid conductor; and

(4) solid-to-ambient conductor.

A typical flow network for conjugate heat transfer is shown in Figure 13.

The energy conservation equation for the solid node is solved in conjunction with all other conservation equations. The energy conservation for the solid node can be expressed as follows (Cross *et al.*, 2002):

$$\frac{(mC_pT_w)_{t+\Delta t} - (mC_pT_w)_t}{\Delta t} = -h_cA(T_w - T_f), \tag{9}$$

where h_c is the heat transfer coefficient, T_w the wall temperature, and T_f the fluid temperature. In this test problem, a constant heat transfer coefficient has been used for comparison with the analytical solution. In our numerical implementations, equation (9) is solved by either successive substitution or Newton's method for the solid temperature for the given fluid temperature and then is repeated until convergence.

For numerical simulations, a copper tube was selected that is 200 ft long, has a 5/8-in inside diameter, and is initially at a temperature of $T_{w,0} = 44.334\,^{\circ}\mathrm{F}$. The tube is then chilled by hydrogen entering the tube at $T_{f,0} = -200\,^{\circ}\mathrm{F}$ and 75 psia. The pressure at the outlet is set at 13.3 psia.

4.2.1 Cryogenic chilldown analytical model. Consider a situation where hydrogen, at temperature $T_{f,0}$, enters a circular tube, whose temperature is $T_{w,0}$. The flow is assumed to be one dimensional with fluid velocity in the axial direction only. Further, assuming that:

- axial conduction in the fluid can be neglected;
- fluid mass flow rate is constant;

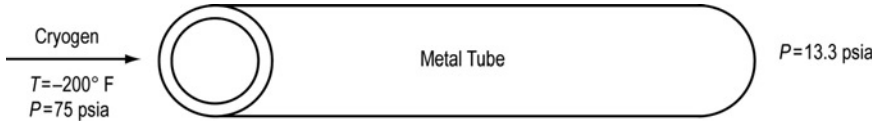

Figure 12.
Schematic of the cryogenic pipeline

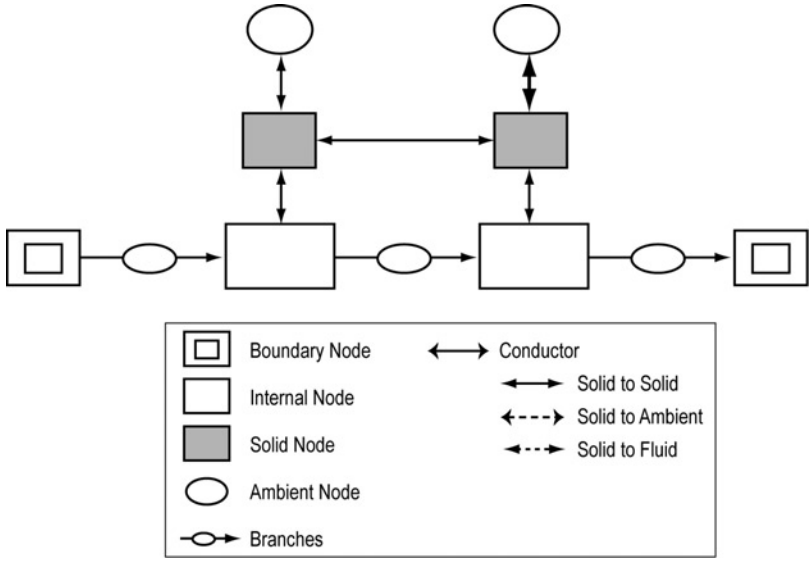

Figure 13.
A schematic showing the connection of a solid node with neighboring solid, fluid, and ambient nodes

- flow work can be neglected;
- heat transfer coefficient is constant; and
- solid and fluid properties are constant, it can be shown (Greyvenstein and Laurie, 1994) that the conservation of energy equations are:

$$h(T_w - T_f) - \frac{C_f \dot{m}}{\pi D}\frac{\partial T_f}{\partial x} = \frac{A_{cc}\rho_f C_f}{\pi D}\frac{\partial T_f}{\partial t}, \tag{10}$$

and

$$\rho_w C_w \delta \frac{dT_w}{dt} = h(T_f - T_w)\ . \tag{11}$$

The coupled system of differential equations (10) and (11), together with the initial and boundary conditions at $t = 0$, $T_w = T_{w,0}$ for all z and at $z = 0$, $T_f = T_{f,0}$ for all t, are solved numerically by discretizing them using a finite difference method. Fourth-order Runge-Kutta difference scheme (Butcher, 1987) is used for the time derivatives discretization, while a backward difference discretization is used for the spatial derivatives.

4.2.2 Results. The conjugate heat transfer problem shown in Figure 12 was simulated with a finite volume model consisting of 33 nodes and 32 branches (Figure 14). Each branch is a pipe flow branch with a length of 80 in and a diameter of 0.625 in. Nodes 1 and 33 are boundary nodes where inlet and outlet conditions were specified. Flow temperatures and pressures were calculated at internal nodes 2-32,

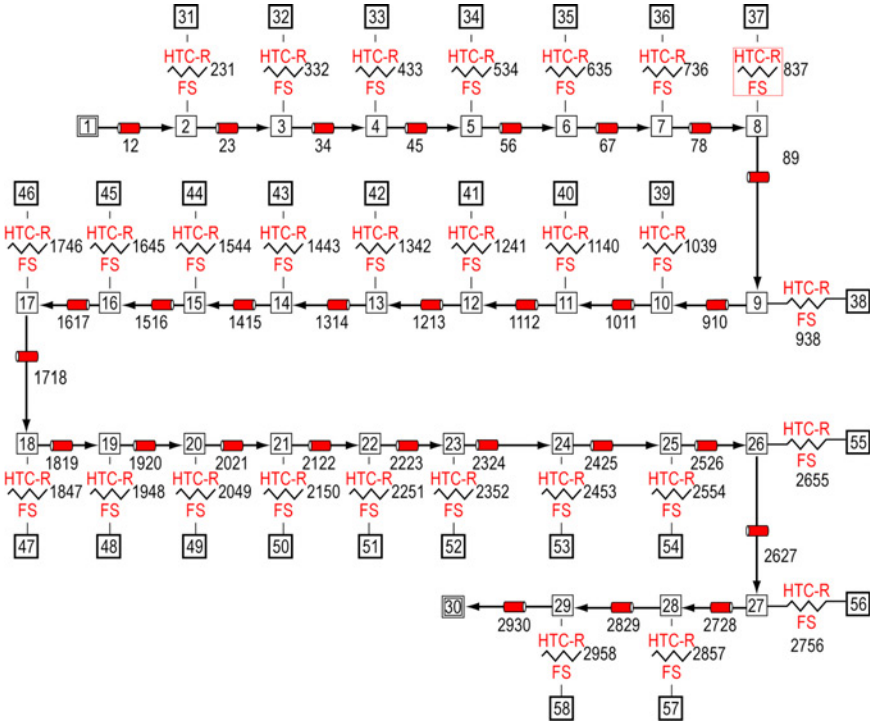

Figure 14.
Finite volume GFSSP model of the flow network for the cryogenic pipeline

which all have an initial temperature of $T_{w,0} = 44.334\,^{\circ}\mathrm{F}$. Each internal node was connected to each other using solid-solid conductors. The solid nodes were also connected to each other using solid-solid conductors. Each solid node has a mass of 3.475 lbm, an initial temperature of 44.334 °F, and has user-defined thermal conductivity. The specific heat value of each solid node is 0.093 Btu/lbm-R. Each solid-fluid conductor has a heat transfer area of 157.07 in^2. However, for comparing the numerical results of the network solvers with the analytical results, a constant value $h = 0.125$ Btu/s/ft^2/°F is used for the heat transfer coefficient. The conduction area and the distance for each solid-solid conductor are 0.477 in^2 and 80 in, respectively.

Figures 15-18 show a comparison of fluid and solid wall temperatures computed using the analytical model (Cross *et al.*, 2002) with temperatures determined by the four nonlinear network solvers. The analytical model uses a constant fluid properties and

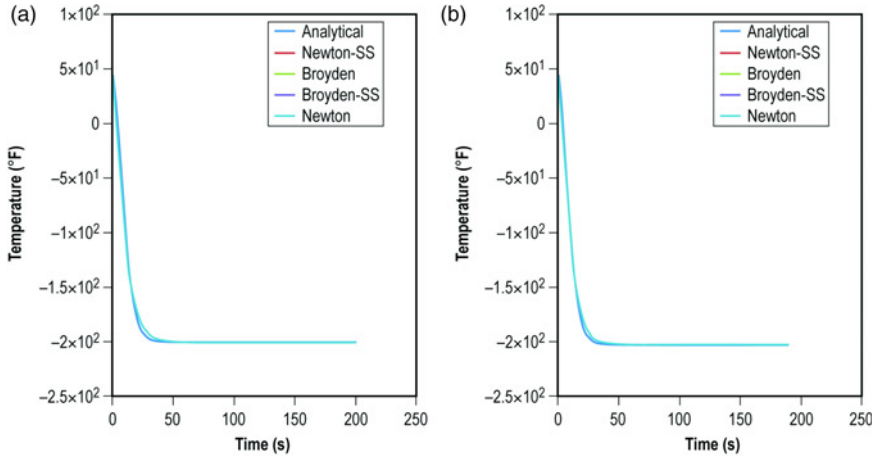

Note: Temperature history computed with various solvers and analytical model

Figure 15.
Comparison of (a) fluid and (b) solid temperature measured at a station located 13.34 ft from the entrance

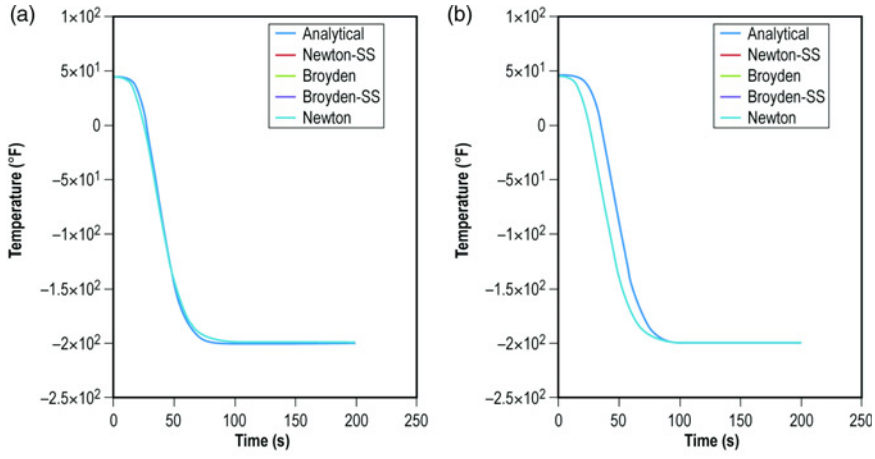

Note: Temperature history computed with various solvers and analytical model

Figure 16.
Comparison of (a) fluid and (b) solid temperature measured at a station located 80 ft from the entrance

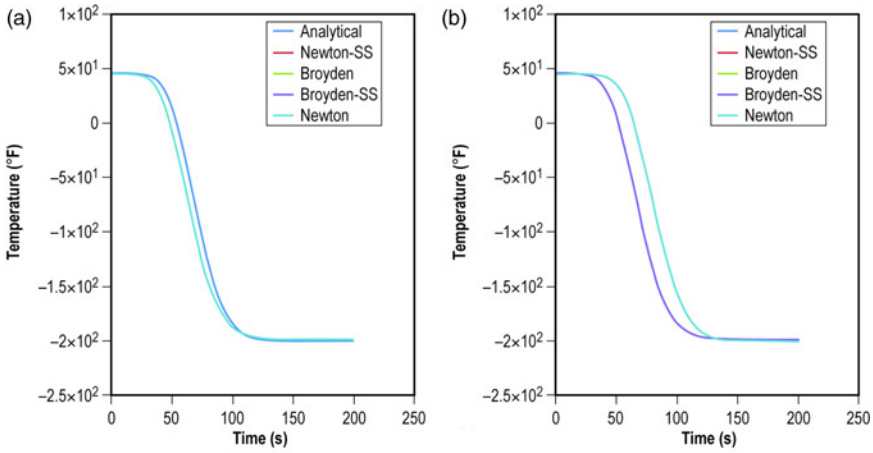

Notes: Temperature history computed with various solvers and analytical model

Figure 17.
Comparison of (a) fluid and (b) solid temperature measured at a station located 148.67 ft from the entrance

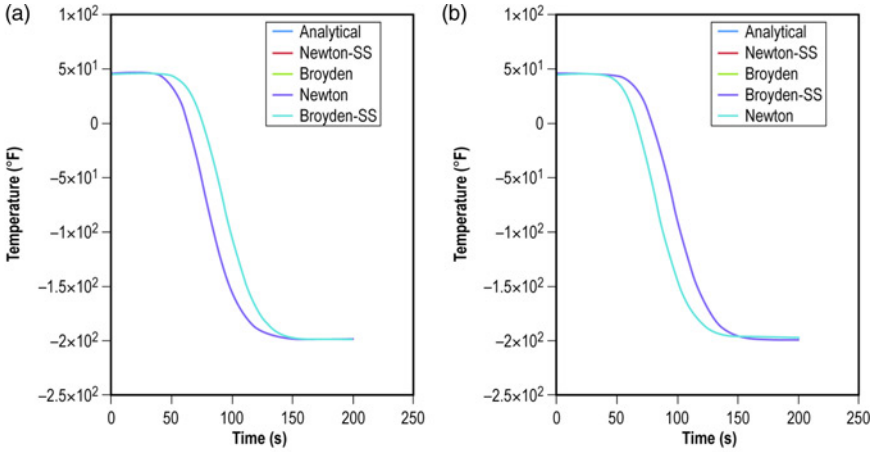

Notes: Temperature history computed with various solvers and analytical model

Figure 18.
Comparison of (a) fluid and (b) solid temperature measured at a station located 186.67 ft from the entrance

mass flow rate, whereas in nonlinear network solvers, these quantities are allowed to vary. In spite of these differences, the computed quantities have very good agreement in general. Table V presents the CPU time taken by the four nonlinear solvers with the tolerance of 10^{-8}. The Broyden-SS solver takes the least amount of CPU time and yet

Fluid	Solid	
	Newton (s)	Successive substitution (s)
Newton	4,254	3,920
Broyden	1,843	1,280
Newton-SS	1,153	661
Broyden-SS	1,164	650

Table V.
CPU time comparison with various solvers used to solve the conjugate heat transfer model with tolerance $=10^{-8}$

produces results that are as accurate as the other three solvers. These observations are reconfirmed by a simulation run with the tolerance of 10^{-6}, as shown in Table VI. The results in Table VI also reveal that use of smaller (tighter) tolerance is not essential for all the problems, especially with the Broyden solvers. CPU experiments performed with these solvers reported in this paper, and others that are not reported here, unequivocally show that nonlinear solvers are reliable in numerically solving the chilldown problem.

5. Conclusions

Fast, nonlinear solvers have been developed in a finite volume-based network flow analysis program for fast and accurate predictions of fluid and thermal transients. The proposed numerical method's ability to predict fluid and thermal transients accurately has been demonstrated by solving two important transient problems:

(1) the water hammer problem which involves a rapid valve closure in a long cryogenic pipeline; and

(2) the chilldown problem in a cryogenic transfer line. Comparisons were made in each case with analytical results, and most showed good agreement.

These agreements establish the viability of the nonlinear solvers to predict the fluid and thermal transients for design of the propulsion system fluid network.

A judicious selection of nonlinear solvers to solve individual conservation equations has been found to be a key element in improving CPU efficiency of the overall scheme. It is preferable to use the simultaneous solver of Newton or Broyden to solve the mass and momentum conservation equations and thermodynamic equation of state because of the strong coupling between pressure, flow rate, and resident mass of the control volume. For most problems, the energy conservation equation can be solved by successive substitution (fixed-point iteration method) for improved efficiency. For both types of problems stated in this paper, a combination of the Broyden and successive substitution method is found to be superior to a combination of the Newton and successive substitution method.

References

Abott, M.B. (1966), *An Introduction to the Method of the Characteristics*, Elsevier, New York, NY.

Broyden, C.G. (1965), "A class of methods for solving nonlinear simultaneous equations", *Mathematics of Computation*, Vol. 19, pp. 577-93.

Butcher, J.C. (1987), *The Numerical Analysis of Ordinary Differential Equations, Runge-Kutta and General Linear Methods*, Wiley, Chichester and New York, NY.

Chaudhry, M.H. (1979), *Applied Hydraulic Transients*, Van Nostrand Reinhold Co, New York, NY, pp. 44-73.

Table VI.
CPU time comparison with various solvers used to solve the conjugate heat transfer models with tolerance $=10^{-6}$

Fluid	Solid	
	Newton (s)	Successive Substitution (s)
Newton	3,878	972
Broyden	1,371	966
Newton-SS	941	471
Broyden-SS	823	452

Chi, J.W.H. (1965), "Cooldown temperatures and cooldown time during mist flow", *Advances in Cryogenic Engineering*, Vol. 10, pp. 330-40.

Colebrook, C.F. (1938-1939), "Turbulent flow in pipes, with particular reference to the transition between the smooth and rough pipe laws", *Journal of Institute of Civil Engineering (London)*, Vol. 11, pp. 133-56.

Cross, M.F., Majumdar, A.K., Bennett Jr., J.C. and Malla, R.B. (2002), "Modeling of chilldown in cryogenic transfer lines", *Journal of Spacecraft and Rockets*, Vol. 39 No. 2, pp. 284-9.

Greyvenstein, G.P. and Laurie, D.P. (1994), "A segregated CFD approach to pipe network analysis", *International Journal of Numerical Methods in Engineering*, Vol. 37, pp. 3685-705.

Hendricks, R.C., Baron, A.K. and Peller, I.C. (1975), "GASP – a computer code for calculating the thermodynamic and transport properties for ten fluids: parahydrogen, helium, neon, methane, nitrogen, carbon monoxide, oxygen, fluorine, argon, and carbon dioxide", NASA TN D-7808, Washington, DC.

Kelly, C.T. (1995), *Iterative Methods for Linear and Nonlinear Equations, Frontiers in Applied Mathematics*, SIAM, Philadelphia, PA.

Majumdar, A.K. (1999), "A second law based unstructured finite volume procedure for generalized flow simulation", *Proceedings of the 37th AIAA Aerospace Sciences Meeting Conference and Exhibit, Reno, NV, 11-14 January.*

Majumdar, A.K. and Flachbart, R.H. (2003), "Numerical modeling of fluid transients by a finite volume procedure for rocket propulsion systems", *Proceedings of the ASME FEDSM'03, Fourth ASME/JSME Joint Fluids Engineering Conference, Honolulu, HI, 6-10 July.*

Majumdar, A.K. and Steadman, T. (2001), "Numerical modeling of pressurization of a propellant tank", *Journal of Propulsion and Power*, Vol. 17 No. 2, pp. 385-90.

Moody, F.J. (1990), *Introduction to Unsteady Thermofluid Mechanics*, John Wiley & Sons, New York, NY, pp. 408-22.

Osiadacz, A.J. (1988), "Methods of steady state simulation of a gas network", *International Journal of Systems Science*, Vol. 19 No. 11, pp. 2395-405.

Patankar, S.V. (1980), *Numerical Heat Transfer*, Hemisphere Publishing Cooperation, Washington, DC.

Patankar, S.V. and Spalding, D.B. (1972), "A calculation procedure for heat, mass and momentum transfer in three-dimensional parabolic flows", *International Journal of Heat Mass Transfer*, Vol. 15, pp. 1787-803.

Steward, W.G., Smith, R.V. and Brennan, J.A. (1970), "Cool down transients in cryogenic transfer lines", *Advances in Cryogenic Engineering*, Vol. 15, pp. 354-63.

Stuttaford, P.J. and Rubini, P.A. (1996), "Preliminary gas turbine combustor design using a network approach", *Int. Gas Turbine and Aeroengine Congress & Exhibition, Birmingham, 10-13 June, ASME 96-GT-135*.

Wylie, E.B. and Streeter, V. (1982), *Fluid Transients*, FEB Press, Ann Arbor, MI, pp. 13-61.

About the authors

Alok K. Majumdar is an Aerospace Technologist, Thermal and Combustion Analysis Branch and Member of AIAA.

S.S. Ravindran is an Associate Professor, Department of Mathematical Sciences and Member of ASME. S.S. Ravindran is the corresponding author and can be contacted at: ravinds@uah.edu